6-2018

Observation of $e^+e^- \to \pi^+\pi^-\pi^0\chi_{b1,2}(1P)$ and search for $e^+e^- \to \phi\chi_{b1,2}(1P)$ at $\sqrt{s}$ =10.96—11.05 GeV

J. H. Yin et al.
Belle Collaboration

Ratnappuli L. Kulasiri
Kennesaw State University, rkulasir@kennesaw.edu

Observation of $e^+e^- \to \pi^+\pi^-\pi^0\chi_{b1,2}(1P)$ and search for $e^+e^- \to \phi\chi_{b1,2}(1P)$ at $\sqrt{s}$ =10.96—11.05 GeV

J. H. Yin,[27] C. Z. Yuan,[27] I. Adachi,[18,14] H. Aihara,[86] S. Al Said,[79,37] D. M. Asner,[4] V. Aulchenko,[5,66] T. Aushev,[55] R. Ayad,[79] V. Babu,[80] I. Badhrees,[79,36] S. Bahinipati,[22] A. M. Bakich,[78] V. Bansal,[68] P. Behera,[25] C. Beleño,[13] B. Bhuyan,[23] T. Bilka,[6] J. Biswal,[33] A. Bobrov,[5,66] A. Bozek,[63] M. Bračko,[49,33] T. E. Browder,[17] L. Cao,[34] D. Červenkov,[6] P. Chang,[62] V. Chekelian,[50] A. Chen,[60] B. G. Cheon,[16] K. Chilikin,[44] K. Cho,[38] S.-K. Choi,[15] Y. Choi,[77] S. Choudhury,[24] D. Cinabro,[90] S. Cunliffe,[9] N. Dash,[22] S. Di Carlo,[42] J. Dingfelder,[3] Z. Doležal,[6] T. V. Dong,[18,14] Z. Drásal,[6] S. Eidelman,[5,66,44] D. Epifanov,[5,66] J. E. Fast,[68] T. Ferber,[9] B. G. Fulsom,[68] R. Garg,[69] V. Gaur,[89] N. Gabyshev,[5,66] A. Garmash,[5,66] M. Gelb,[34] A. Giri,[24] P. Goldenzweig,[34] B. Golob,[45,33] J. Haba,[18,14] K. Hayasaka,[65] H. Hayashii,[59] S. Hirose,[56] W.-S. Hou,[62] T. Iijima,[57,56] K. Inami,[56] G. Inguglia,[9] A. Ishikawa,[84] R. Itoh,[18,14] M. Iwasaki,[67] Y. Iwasaki,[18] W. W. Jacobs,[26] I. Jaegle,[10] H. B. Jeon,[41] S. Jia,[2] Y. Jin,[86] D. Joffe,[35] K. K. Joo,[7] T. Julius,[51] K. H. Kang,[41] T. Kawasaki,[65] C. Kiesling,[50] D. Y. Kim,[75] J. B. Kim,[39] K. T. Kim,[39] S. H. Kim,[16] K. Kinoshita,[8] P. Kodyš,[6] S. Korpar,[49,33] D. Kotchetkov,[17] P. Križan,[45,33] R. Kroeger,[52] P. Krokovny,[5,66] T. Kuhr,[46] R. Kulasiri,[35] Y.-J. Kwon,[92] J. S. Lange,[12] I. S. Lee,[16] S. C. Lee,[41] L. K. Li,[27] Y. B. Li,[70] L. Li Gioi,[50] J. Libby,[25] D. Liventsev,[89,18] M. Lubej,[33] T. Luo,[11] M. Masuda,[85] T. Matsuda,[53] D. Matvienko,[5,66,44] M. Merola,[30,58] H. Miyata,[65] R. Mizuk,[44,54,55] G. B. Mohanty,[80] H. K. Moon,[39] T. Mori,[56] R. Mussa,[31] E. Nakano,[67] T. Nanut,[33] K. J. Nath,[23] Z. Natkaniec,[63] M. Nayak,[90,18] M. Niiyama,[40] N. K. Nisar,[71] S. Nishida,[18,14] K. Nishimura,[17] K. Ogawa,[65] S. Ogawa,[83] H. Ono,[64,65] P. Pakhlov,[44,54] G. Pakhlova,[44,55] B. Pal,[4] S. Pardi,[30] H. Park,[41] S. Paul,[82] T. K. Pedlar,[47] R. Pestotnik,[33] L. E. Piilonen,[89] V. Popov,[44,55] E. Prencipe,[20] A. Rostomyan,[9] G. Russo,[30] D. Sahoo,[80] Y. Sakai,[18,14] M. Salehi,[48,46] S. Sandilya,[8] L. Santelj,[18] T. Sanuki,[84] V. Savinov,[71] O. Schneider,[43] G. Schnell,[1,21] C. Schwanda,[28] Y. Seino,[65] K. Senyo,[91] O. Seon,[56] M. E. Sevior,[51] C. P. Shen,[2] T.-A. Shibata,[87] J.-G. Shiu,[62] B. Shwartz,[5,66] F. Simon,[50,81] A. Sokolov,[29] E. Solovieva,[44,55] M. Starič,[33] T. Sumiyoshi,[88] W. Sutcliffe,[34] M. Takizawa,[74,19,72] U. Tamponi,[31] K. Tanida,[32] F. Tenchini,[51] M. Uchida,[87] T. Uglov,[44,55] Y. Unno,[16] S. Uno,[18,14] P. Urquijo,[51] C. Van Hulse,[1] R. Van Tonder,[34] G. Varner,[17] A. Vinokurova,[5,66] V. Vorobyev,[5,66,44] B. Wang,[8] C. H. Wang,[61] M.-Z. Wang,[62] P. Wang,[27] X. L. Wang,[11] S. Watanuki,[84] E. Widmann,[76] E. Won,[39] H. Yamamoto,[84] H. Ye,[9] Y. Yusa,[65] Z. P. Zhang,[73] V. Zhilich,[5,66] V. Zhukova,[44,54] and V. Zhulanov[5,66]

(The Belle Collaboration)

[1]*University of the Basque Country UPV/EHU, 48080 Bilbao*

[2]*Beihang University, Beijing 100191*

[3]*University of Bonn, 53115 Bonn*

[4]*Brookhaven National Laboratory, Upton, New York 11973*

[5]*Budker Institute of Nuclear Physics SB RAS, Novosibirsk 630090*

[6]*Faculty of Mathematics and Physics, Charles University, 121 16 Prague*

[7]*Chonnam National University, Kwangju 660-701*

[8]*University of Cincinnati, Cincinnati, Ohio 45221*

[9]*Deutsches Elektronen–Synchrotron, 22607 Hamburg*

[10]*University of Florida, Gainesville, Florida 32611*

[11]*Key Laboratory of Nuclear Physics and Ion-beam Application (MOE) and Institute of Modern Physics, Fudan University, Shanghai 200443*

[12]*Justus-Liebig-Universität Gießen, 35392 Gießen*

[13]*II. Physikalisches Institut, Georg-August-Universität Göttingen, 37073 Göttingen*

[14]*SOKENDAI (The Graduate University for Advanced Studies), Hayama 240-0193*

[15]*Gyeongsang National University, Chinju 660-701*

[16]*Hanyang University, Seoul 133-791*

[17]*University of Hawaii, Honolulu, Hawaii 96822*

[18]*High Energy Accelerator Research Organization (KEK), Tsukuba 305-0801*

[19]*J-PARC Branch, KEK Theory Center, High Energy Accelerator Research Organization (KEK), Tsukuba 305-0801*

[20]*Forschungszentrum Jülich, 52425 Jülich*

[21]*IKERBASQUE, Basque Foundation for Science, 48013 Bilbao*

[22]*Indian Institute of Technology Bhubaneswar, Satya Nagar 751007*

[23]*Indian Institute of Technology Guwahati, Assam 781039*

[24]*Indian Institute of Technology Hyderabad, Telangana 502285*

[25]*Indian Institute of Technology Madras, Chennai 600036*

[26]*Indiana University, Bloomington, Indiana 47408*

[27]*Institute of High Energy Physics, Chinese Academy of Sciences, Beijing 100049*

[28]*Institute of High Energy Physics, Vienna 1050*

[29]*Institute for High Energy Physics, Protvino 142281*

[30]*INFN - Sezione di Napoli, 80126 Napoli*

[31]*INFN - Sezione di Torino, 10125 Torino*

[32]*Advanced Science Research Center, Japan Atomic Energy Agency, Naka 319-1195*

[33]*J. Stefan Institute, 1000 Ljubljana*

[34]*Institut für Experimentelle Teilchenphysik, Karlsruher Institut für Technologie, 76131 Karlsruhe*

[35]*Kennesaw State University, Kennesaw, Georgia 30144*

[36]*King Abdulaziz City for Science and Technology, Riyadh 11442*

[37]*Department of Physics, Faculty of Science, King Abdulaziz University, Jeddah 21589*

[38]*Korea Institute of Science and Technology Information, Daejeon 305-806*

[39]*Korea University, Seoul 136-713*

[40]*Kyoto University, Kyoto 606-8502*

[41]*Kyungpook National University, Daegu 702-701*

[42]*LAL, Univ. Paris-Sud, CNRS/IN2P3, Université Paris-Saclay, Orsay*

[43]*École Polytechnique Fédérale de Lausanne (EPFL), Lausanne 1015*

[44]*P.N. Lebedev Physical Institute of the Russian Academy of Sciences, Moscow 119991*

[45]*Faculty of Mathematics and Physics, University of Ljubljana, 1000 Ljubljana*

[46]*Ludwig Maximilians University, 80539 Munich*

[47]*Luther College, Decorah, Iowa 52101*

[48]*University of Malaya, 50603 Kuala Lumpur*

[49]*University of Maribor, 2000 Maribor*

[50]*Max-Planck-Institut für Physik, 80805 München*

[51]*School of Physics, University of Melbourne, Victoria 3010*

[52]*University of Mississippi, University, Mississippi 38677*

[53]*University of Miyazaki, Miyazaki 889-2192*

[54]*Moscow Physical Engineering Institute, Moscow 115409*

[55]*Moscow Institute of Physics and Technology, Moscow Region 141700*

[56]*Graduate School of Science, Nagoya University, Nagoya 464-8602*

[57]*Kobayashi-Maskawa Institute, Nagoya University, Nagoya 464-8602*

[58]*Università di Napoli Federico II, 80055 Napoli*

[59]*Nara Women's University, Nara 630-8506*

[60]*National Central University, Chung-li 32054*

[61]*National United University, Miao Li 36003*

[62]*Department of Physics, National Taiwan University, Taipei 10617*

[63]*H. Niewodniczanski Institute of Nuclear Physics, Krakow 31-342*

[64]*Nippon Dental University, Niigata 951-8580*

[65]*Niigata University, Niigata 950-2181*

[66]*Novosibirsk State University, Novosibirsk 630090*

[67]*Osaka City University, Osaka 558-8585*

[68]*Pacific Northwest National Laboratory, Richland, Washington 99352*

[69]*Panjab University, Chandigarh 160014*

[70]*Peking University, Beijing 100871*

[71]*University of Pittsburgh, Pittsburgh, Pennsylvania 15260*

[72]*Theoretical Research Division, Nishina Center, RIKEN, Saitama 351-0198*

[73]*University of Science and Technology of China, Hefei 230026*

[74]*Showa Pharmaceutical University, Tokyo 194-8543*

[75]*Soongsil University, Seoul 156-743*

[76]*Stefan Meyer Institute for Subatomic Physics, Vienna 1090*

[77]*Sungkyunkwan University, Suwon 440-746*

[78]*School of Physics, University of Sydney, New South Wales 2006*

[79]*Department of Physics, Faculty of Science, University of Tabuk, Tabuk 71451*

[80]*Tata Institute of Fundamental Research, Mumbai 400005*

[81]*Excellence Cluster Universe, Technische Universität München, 85748 Garching*

[82]*Department of Physics, Technische Universität München, 85748 Garching*

[83]*Toho University, Funabashi 274-8510*

[84]*Department of Physics, Tohoku University, Sendai 980-8578*

[85]*Earthquake Research Institute, University of Tokyo, Tokyo 113-0032*

[86]*Department of Physics, University of Tokyo, Tokyo 113-0033*

[87]*Tokyo Institute of Technology, Tokyo 152-8550*

[88]*Tokyo Metropolitan University, Tokyo 192-0397*

[89]*Virginia Polytechnic Institute and State University, Blacksburg, Virginia 24061*

[90]*Wayne State University, Detroit, Michigan 48202*

[91]*Yamagata University, Yamagata 990-8560*

[92]*Yonsei University, Seoul 120-749*

(Dated: June 19, 2018)

We report searches for the processes $e^+e^- \to \pi^+\pi^-\pi^0\chi_{bJ}$ and $e^+e^- \to \phi\chi_{bJ}$ (J=1,2) in the vicinity of the $\Upsilon(11020)$ resonance using energy scan data collected by the Belle experiment at the KEKB collider. We observe $e^+e^- \to \pi^+\pi^-\pi^0\chi_{b1}$ and find evidence for $e^+e^- \to \omega\chi_{b2}$ processes for data with center-of-mass energies from 10.96 to 11.05 GeV for the first time. The statistical significance for $\pi^+\pi^-\pi^0\chi_{b1}$ and $\omega\chi_{b2}$ are 6.1σ and 4.0σ, respectively. We investigate energy dependence of the $e^+e^- \to \pi^+\pi^-\pi^0\chi_{bJ}$ cross section and find that it is consistent with production of $\Upsilon(10860)$ and $\Upsilon(11020)$ resonances without significant non-resonant contribution. Assuming $e^+e^- \to \pi^+\pi^-\pi^0\chi_{bJ}$ proceeds via $\Upsilon(10860)$ and $\Upsilon(11020)$, the branching fraction $\mathcal{B}(\Upsilon(11020) \to \pi^+\pi^-\pi^0\chi_{bJ}) = (8.6 \pm 4.1 \pm 6.1^{+4.5}_{-2.5}) \times 10^{-3}$ is measured for the first time, where the first error is statistical, the second is systematic, and the third from the branching fraction of $\Upsilon(11020) \to e^+e^-$. The signals for $e^+e^- \to \phi\chi_{bJ}$ are not significant, and the upper limits of the Born cross sections at the 90% confidence level are 0.6 and 1.0 pb for $e^+e^- \to \phi\chi_{b1}$ and $\phi\chi_{b2}$, respectively, for center-of-mass energies from 10.96 to 11.05 GeV.

PACS numbers: 13.25.Gv, 12.38.-t

Hadronic transitions among heavy quarkonium states serve as a key source of information for better understanding of the strong interaction between a quark-antiquark pair, and thus quantum chromodynamics (QCD). The heavy quarkonium

systems are in general non-relativistic and the hadronic transitions to lower lying states have long been described using the QCD multipole expansion [1]. However, the existence of anomalously large hadronic transition rates from the $\Upsilon(10860)$ as reported by the Belle experiment [2–9] challenge the theoretical calculations as well as the pure bottomonium nature of the $\Upsilon(10860)$ and $\Upsilon(11020)$ [10–12].

The processes $e^+e^- \to \omega\chi_{bJ}$ were observed recently [4] using data samples taken at energies near the $\Upsilon(10860)$ peak, but the dependence of the $e^+e^- \to \omega\chi_{bJ}$ cross section versus energy was not measured. Therefore, it is unclear whether this process occurs from resonant $\Upsilon(10860)$ or continuum process. Nevertheless, the result has been investigated extensively by theorists to understand the dynamics of these transitions, producing studies of S- and D-wave mixing for the observed heavy quark symmetry violation between $\omega\chi_{b1}$ and $\omega\chi_{b2}$ [13], the possible contribution of $\Upsilon(10860) \to \pi Z_b \to \pi\rho\Upsilon(1S)$ [14], a molecular component in the $\Upsilon(10860)$ wave function [14], and hadronic loop effects [15].

By extending the calculation used in Ref. [15] to the $\Upsilon(11020)$ case, authors of Ref. [16] predict the branching fractions for $\Upsilon(11020) \to \omega\chi_{bJ}$ to be $(0.15 \sim 2.81) \times 10^{-3}$, $(0.63 \sim 11.68) \times 10^{-3}$, and $(1.08 \sim 20.02) \times 10^{-3}$, for $J = 0, 1,$ and 2, respectively. In addition, the branching fractions of $\Upsilon(11020) \to \phi\chi_{bJ}$ are also predicted, yielding $(0.68 \sim 4.62) \times 10^{-6}$, $(0.50 \sim 3.43) \times 10^{-6}$, and $(2.22 \sim 15.18) \times 10^{-6}$, for $J = 0, 1,$ and 2, respectively. The measurement of these ω and ϕ transitions will test theoretical calculations and offer insight into the nature of the $\Upsilon(11020)$ and its decay dynamics.

In this Letter, we report the results of a search for $\Upsilon(11020) \to \omega\chi_{bJ}$ and $\phi\chi_{bJ}$ using the $\Upsilon(10860)$ and $\Upsilon(11020)$ energy scan data collected with the Belle detector. Hereinafter, the $\Upsilon(10860)$ and $\Upsilon(11020)$ are referred to, for brevity, as the $\Upsilon(5S)$ and $\Upsilon(6S)$ according to the potential model assignment. The data that we are using consist of 121.4 fb^{-1} from three energy points near the $\Upsilon(5S)$ peak, 19 data samples with integrated luminosity of about 1 fb^{-1} per point, and 18 data samples of about 50 pb^{-1} per point taken in 5 MeV steps between 10.96 and 11.05 GeV [17]. The corresponding luminosities of the $\Upsilon(5S)$ peak data and the 19 samples with high luminosities are listed in Table I as well as the center of mass (c.m.) energies. We use $\chi_{bJ} \to \gamma\Upsilon(1S)$, $\Upsilon(1S) \to \ell^+\ell^-$ ($l = e,\ \mu$), $\omega \to \pi^+\pi^-\pi^0$ to reconstruct the $e^+e^- \to \omega\chi_{b1,2}$ signal; while for $e^+e^- \to \phi\chi_{bJ}$ signal, we reconstruct ϕ with its decays to K^+K^- and determine transitions to χ_{bJ} by studying the K^+K^- recoil mass.

The Belle detector, located at the KEKB asymmetric-energy e^+e^- collider [18] is described in Ref. [19]. The EVTGEN [20] generator is used to produce simulated events using Monte Carlo (MC) mothods. The nominal parameters of the states in the decay chains are quoted from Ref. [21]. To take the initial state radiation (ISR) into consideration, we use the VECTORISR model [20] in EVTGEN. Generic MC samples at $\Upsilon(5S)$ peak and continuum data, taken at 10.52 GeV, are also used to study the background shape.

TABLE I. Energy-dependent Born cross sections for $e^+e^- \to \pi^+\pi^-\pi^0\chi_{bJ}$ at different c.m. energy (in GeV) with corresponding integrated luminosity.

$E_{c.m.}$ (GeV)	$\mathcal{L}$(fb^{-1})	$\sigma^B(\pi^+\pi^-\pi^0\chi_{bJ})$ (pb)
10.7711	0.955	$-1.36^{+2.47}_{-1.64}$
10.8203	1.164	$2.73^{+2.08}_{-1.43}$
10.8497	0.989	$2.57^{+2.08}_{-1.35}$
10.8589	0.989	$0.64^{+1.53}_{-0.76}$
10.8633	47.648	$0.83^{+0.11}_{-0.11}$
10.8667	45.553	$0.68^{+0.10}_{-0.10}$
10.8686	22.938	$0.89^{+0.16}_{-0.16}$
10.8695	0.978	$1.30^{+2.06}_{-1.28}$
10.8785	0.978	$1.92^{+1.92}_{-1.18}$
10.8836	1.230	$1.46^{+1.66}_{-1.07}$
10.8889	0.989	$1.22^{+1.65}_{-0.94}$
10.8985	0.983	$1.15^{+1.56}_{-0.88}$
10.9011	0.873	$-1.26^{+1.83}_{-1.07}$
10.9077	0.980	$0.53^{+1.54}_{-0.90}$
10.9275	0.667	$1.94^{+1.94}_{-0.90}$
10.9575	0.851	$0.70^{+1.65}_{-0.82}$
10.9775	0.999	$2.97^{+2.06}_{-1.38}$
10.9919	0.986	$1.16^{+1.57}_{-0.89}$
11.0068	0.976	$3.12^{+1.90}_{-1.31}$
11.0164	0.771	$3.59^{+2.19}_{-1.51}$
11.0175	0.849	$0.00^{+0.99}_{-0.33}$
11.0220	0.982	$0.89^{+1.57}_{-1.03}$

For charged tracks, the impact parameters perpendicular to and along the beam direction with respect to the interaction point are required to be less than 1.0 and 3.5 cm, respectively. The transverse momentum is restricted to be higher than 0.1 GeV/c. A likelihood $\mathcal{L}(X)$ for each charged track is obtained from different detector subsystems for a particle hypothesis $X \in e, \mu, \pi, K, p$ (PID). Tracks with a likelihood ratio $\mathcal{R}(K) = \mathcal{L}(K)/(\mathcal{L}(K) + \mathcal{L}(\pi)) < 0.4$ are identified as pions while those with $\mathcal{R}(K) > 0.6$ are identified as kaons. Similarly, we define the likelihood ratios $\mathcal{R}(e)$ and $\mathcal{R}(\mu)$ for identification of electrons and muons, respectively, with $\mathcal{R}(e) > 0.01$ and $\mathcal{R}(\mu) > 0.1$. A neutral cluster in the electromagnetic calorimeter is reconstructed as a photon if it does not match the extrapolated position of any charged track and its energy is greater than 30 MeV.

To select $e^+e^- \to \pi^+\pi^-\pi^0\chi_{bJ}$ candidates, we require that there be exactly four tracks, of which two are positively identified as pions and the other two as leptons. At least three photons are required in the event and a π^0-list is created with invariant mass of the photon pairs satisfying $M(\gamma\gamma) \in [0.12,\ 0.15]$ GeV/c^2, which covers nearly $\pm 3\sigma$ around the π^0 peak. To improve momentum resolution, photon energy resolution, and reduce background, a five-constraint (5C) kinematic fit is performed, where the invariant mass of the π^0 candidate is constrained to be the nominal mass and the energy and momentum of the final state system are constrained to those of the initial e^+e^- system. The momenta after the 5C kinematic fit are kept for further analysis. The $\chi^2_{\mathrm{5C}}/\mathrm{ndf}$ is required to be less than 20 for both $\Upsilon(1S) \to \mu^+\mu^-$ and e^+e^- modes. Here $\mathrm{ndf} = 5$ is the number of degrees of

freedom. If there are multiple π^0 combinations in an event, the one with the smallest $\chi^2_{\rm 5C}$/ndf is kept. The invariant mass of $\ell^+\ell^-$ is required to be in the region [9.42, 9.60] GeV/c^2.

The χ_{bJ} candidates are reconstructed with the selected $\Upsilon(1S)$ and the photon not in π^0 combination. The invariant mass of $\pi^+\pi^-\pi^0$ ($M(\pi^+\pi^-\pi^0)$) versus that of $\gamma\Upsilon(1S)$ ($M(\gamma\Upsilon(1S)) = M(\gamma\ell^+\ell^-) - M(\ell^+\ell^-) + m_{\Upsilon(1S)}$) is shown in Fig. 1 for the sum of the data samples in the $\Upsilon(6S)$ energy region, which is defined as $E_{\rm c.m.} > 10.96$ GeV. Clusters of events for the production of χ_{bJ} can be seen both when $M(\pi^+\pi^-\pi^0)$ is in ω mass region ([0.75, 0.81] GeV/c^2) and at higher masses (> 0.81 GeV/c^2). For events having $M(\pi^+\pi^-\pi^0)$ in the ω mass region, the χ_{b2} signal is dominant while for signal events with higher $\pi^+\pi^-\pi^0$ masses, the χ_{b1} signal is dominant. Background mainly comes from fake π^0's from photon candidate combinatoric.

An unbinned two-dimensional (2D) extended maximum likelihood fit to $M(\pi^+\pi^-\pi^0)$ and $M(\gamma\Upsilon(1S))$ is applied to extract the numbers of $\omega\chi_{bJ}$ and $\pi^+\pi^-\pi^0\chi_{bJ}$ events. In the fit, the shapes of $\omega\chi_{bJ}$ and $\pi^+\pi^-\pi^0\chi_{bJ}$ obtained from MC simulation are used to describe the signals, and a 2D function $f(x,y) = ax + by$ ($x = M(\gamma\Upsilon(1S))$ and $y = M(\pi^+\pi^-\pi^0)$), is used to fit the background. Here the $\pi^+\pi^-\pi^0\chi_{bJ}$ MC sample is generated assuming $\pi^+\pi^-\pi^0$ follow a phase space (PHSP) distribution, and this process is denoted $(\pi^+\pi^-\pi^0)_{\text{non-}\omega}\chi_{bJ}$. The statistical significance for $\pi^+\pi^-\pi^0\chi_{b1}$ and $\pi^+\pi^-\pi^0\chi_{b2}$, including both ω and non-ω contributions, are 6.4σ and 3.5σ, respectively. The significances are calculated based on the changed likelihood and number of degrees of freedom with or without signals throughout the paper. The signal yields for $\omega\chi_{b1}$ and $(\pi^+\pi^-\pi^0)_{\text{non-}\omega}\chi_{b2}$ are consistent with zero in the fitting results, and thus are set to zero and the fit is repeated. The projections of the fit results for events in χ_{bJ} signal region ($M(\gamma\Upsilon(1S)) \in [9.87, 9.93]$ GeV/c^2), in ω signal region , and higher than ω mass region are also shown in Fig. 1. The signal yields (statistical significances) for $(\pi^+\pi^-\pi^0)_{\text{non-}\omega}\chi_{b1}$ and $\omega\chi_{b2}$ are 19.6 ± 5.3 (6.1σ) and 7.8 ± 3.2 (4.0σ), respectively. We also use other forms as alternative background descriptions, such as the product of two independent second-order polynomial functions, the 2D function with additional correlative component cxy or constant component. Changes in the fit results are negligible.

In order to study the line shape of $\pi^+\pi^-\pi^0\chi_{b1}$ and $\pi^+\pi^-\pi^0\chi_{b2}$ events, we extract the signal yields $N_{\rm sig}$ at each energy scan point. Because of the limited statistics for most energy points, we do not perform a 2D fit as for the summed sample, nor do we separate $\pi^+\pi^-\pi^0$ into ω and non-ω, nor $\gamma\Upsilon(1S)$ into χ_{b1} and χ_{b2}. The number of χ_{bJ} signal events is computed using the formula: $N_{\rm sig} = N_{\rm obs} - N_{\rm side}$, where $N_{\rm obs}$ is the number of events in χ_{bJ} signal region and $N_{\rm side}$ is that in the sideband region. Here the signal region is defined as $M(\gamma\Upsilon(1S)) \in$ [9.852, 9.952] GeV/c^2, while the sideband region is [9.77, 9.82] and [9.98, 10.03] GeV/c^2.

To estimate reconstruction efficiencies (ϵ), a series of MC samples at every energy scan points are generated. Here we assume that all the $\pi^+\pi^-\pi^0\chi_{bJ}$ signals come from $\Upsilon(5S)$ and $\Upsilon(6S)$ decays. In order to estimate the ISR correction factors, we use

$$1+\delta = \frac{\int_{m_0}^{\sqrt{s}} G_{\rm BW}(\sqrt{s}) F(x,s) ds}{G_{BW}(\sqrt{s})},$$

where m_0 is the threshold of $\pi^+\pi^-\pi^0\chi_{bJ}$, $F(x,s)$ is the radiative function [22] and $G_{\rm BW}(\sqrt{s})$ is the Breit-Wigner (BW) function,

$$G_{\rm BW}(\sqrt{s}) = \frac{12\pi\Gamma_{ee}\cdot\mathcal{B}\cdot\Gamma_{\rm tot}}{(s-M^2)^2+M^2\Gamma^2} \times \frac{\Phi(\sqrt{s})}{\Phi(M)},$$

where Γ_{ee} is the partial decay width of $\Upsilon(5S)$ or $\Upsilon(6S) \to e^+e^-$, $\Gamma_{\rm tot}$ is the total width of $\Upsilon(5S)$ or $\Upsilon(6S)$, $\mathcal{B}$ is the corresponding branching fractions of $\Upsilon(5S)$ or $\Upsilon(6S) \to \pi^+\pi^-\pi^0\chi_{bJ}$, Φ is the approximate two-body PHSP factor which is given by assuming that the $\pi^+\pi^-\pi^0$ is a wide resonance. The Born cross sections are calculated with

$$\sigma^{\rm Born} = \frac{N_{\rm sig}}{\epsilon\mathcal{B}_{\rm inter}\mathcal{L}(1+\delta)/\left|1-\Pi\right|^2},$$

where $\mathcal{B}_{\rm inter}$ is the corresponding intermediate decay branching fractions of $\pi^0 \to \gamma\gamma$, $\chi_{bJ} \to \gamma\Upsilon(1S)$, $\Upsilon(1S) \to \ell^+\ell^-$, $\mathcal{L}$ is the integrated luminosity, and $(1/\left|1-\Pi\right|^2)$ is the vacuum polarization factor [23]. A weighted branching fraction $\mathcal{B}_{\rm weighted} = \mathcal{B}(\chi_{b1} \to \gamma\Upsilon(1S))\cdot f + \mathcal{B}(\chi_{b2} \to \gamma\Upsilon(1S))\cdot(1-f)$ is used in calculating the cross sections, where $f = N_1/(N_1+N_2) = 0.74 \pm 0.06$ is the ratio of χ_{b1} in the sample, with N_J being the number of observed events of $\pi^+\pi^-\pi^0\chi_{bJ}$ obtained in Ref. [4]. We also use an alternative ratio that has been obtained in our analysis, $f = 0.72 \pm 0.14$, which agrees with that from Ref. [4] but with larger error.

The energy-dependent cross sections for $e^+e^- \to \pi^+\pi^-\pi^0\chi_{bJ}$ are listed in Table I and plotted in Fig. 2. Assuming the $\pi^+\pi^-\pi^0\chi_{bJ}$ signal comes from $\Upsilon(5S)$ and $\Upsilon(6S)$ decay, a maximum likelihood fit of the cross sections is performed. The likelihood for the three $\Upsilon(5S)$ peak data samples is calculated assuming the Gaussian distribution, while for the other samples, the likelihood is calculated assuming Poisson distribution scaled to the cross section values because of the limited statistics. The fit function is a coherent sum of two BW amplitudes, i.e., $\Upsilon(5S)$ and $\Upsilon(6S)$, and the masses and widths of the $\Upsilon(5S)$ and $\Upsilon(6S)$ are fixed to their world average values [21] while the corresponding branching fractions are left free. The fit results are shown in Fig. 2. Two solutions are found that differ in phase, but the resulting $\Gamma_{ee}\cdot\mathcal{B}$ are nearly the same. The product branching fractions are $\mathcal{B}(\Upsilon(5S) \to e^+e^-)\cdot\mathcal{B}(\Upsilon(5S) \to \pi^+\pi^-\pi^0\chi_{bJ}) = (15.3 \pm 3.7) \times 10^{-9}$, $\mathcal{B}(\Upsilon(6S) \to e^+e^-)\cdot\mathcal{B}(\Upsilon(6S) \to \pi^+\pi^-\pi^0\chi_{bJ}) = (18.3 \pm 9.0) \times 10^{-9}$, where the errors are statistical. We also try to introduce a continuum component into the fit, but its significance is only 1.4σ.

There are several sources of systematic error in the cross section measurements. Most of the uncertainties are similar

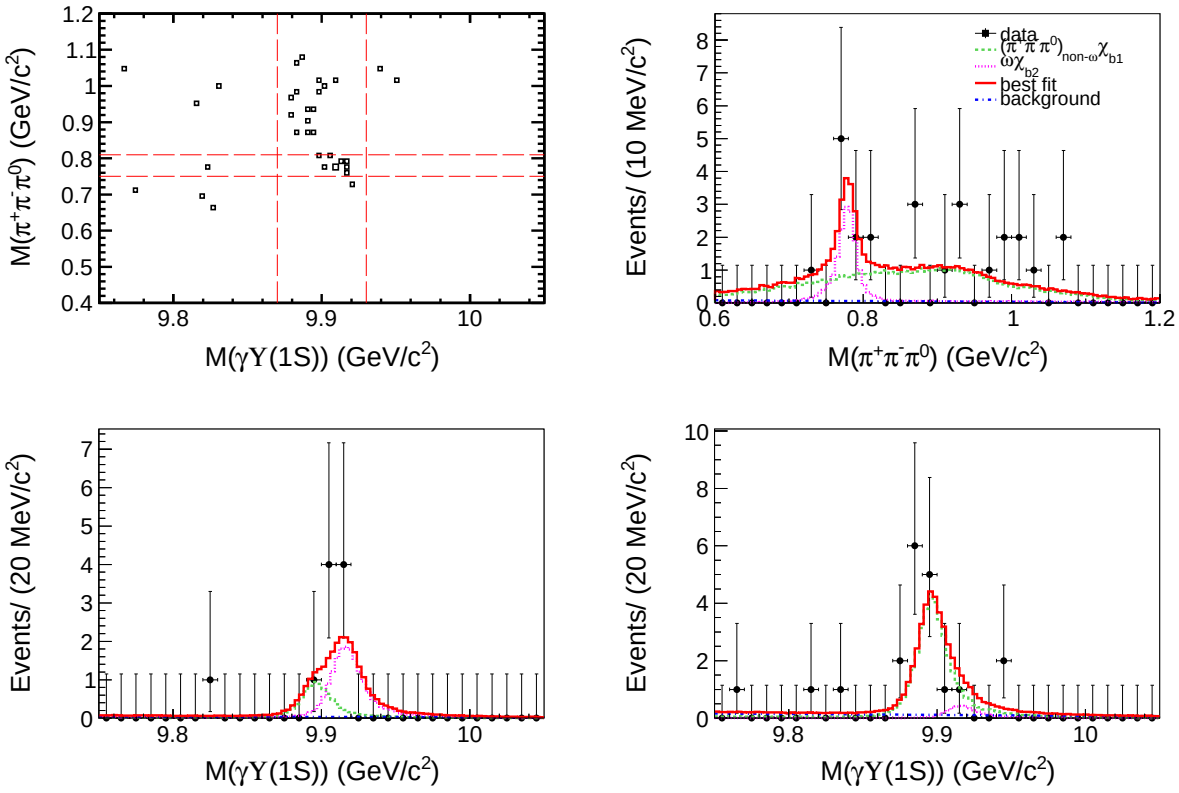

FIG. 1. A scatter plot of $M(\pi^+\pi^-\pi^0)$ versus $M(\gamma\Upsilon(1S))$ from data (top left), and the projections of the 2D fit for events in χ_{bJ} signal region (top right), in ω signal region (bottom left), and out of ω signal region (bottom right). Points with error bars are data, solid lines are the best fit, dashed lines are the χ_{b1} signals, dotted lines are χ_{b2} signals, and the dash-dotted lines are the fitted background.

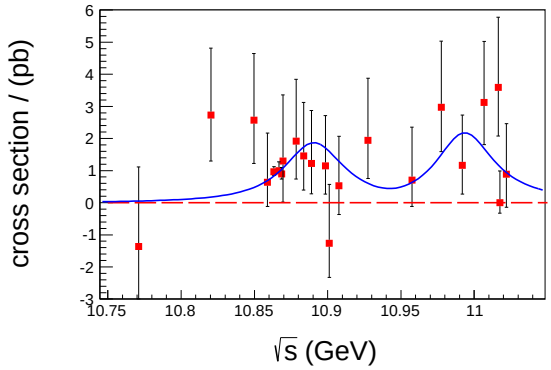

FIG. 2. Fitting to the cross sections of $e^+e^- \to \pi^+\pi^-\pi^0\chi_{bJ}$. Red boxes with error bars are the cross sections of $e^+e^- \to \pi^+\pi^-\pi^0\chi_{bJ}$ and solid blue curve is fitting curve.

to the previous work [4]. The uncertainty from tracking efficiency is 1.0% per pion and kaon track and 0.35% per lepton. The uncertainty from PID efficiency is 1.3% per pion and 1.6% per lepton. The uncertainty in the calibration of the photon energy resolution is less than 1.1%. The uncertainty in the selection of π^0 candidates is estimated by comparing control samples of $\eta \to \pi^0\pi^0\pi^0$ and $\eta \to \pi^+\pi^-\pi^0$ in data, and amounts to 2.2%. The uncertainty due to the 5C kinematic fit is 4.2% and a 3.0% uncertainty is assigned to the trigger simulation. All above systematic uncertainties are quoted from Ref. [4]. The uncertainty from luminosity is 1.5% [9]. Comparing the reconstruction efficiency with the ISR process in EVTGEN and with it removed in the generator, but still corrected for with the ISR correction factor, yields an uncertainty of 1.0% due to the reconstruction efficiency of ISR events. The corresponding uncertainty from the branching fraction is 8.2% quoted from the PDG [21]. The total systematic uncertainty, 11.9%, is obtained by adding all the above results in quadrature.

The systematic uncertainties in the lineshape fit mainly come from the parametrization of the BW function, PHSP factor, resonance parameters, and the fitting function used to describe the line shape. The first is estimated by replacing the constant width with an energy dependent width $\Gamma_{\rm tot} = \Gamma^0_{\rm tot} \cdot \Phi(\sqrt{s})/\Phi(M)$. The second source is estimated by replacing the approximate two-body PHSP factor of $\pi^+\pi^-\pi^0\chi_{bJ}$ with the two-body PHSP factor of $\omega\chi_{bJ}$. The third source is estimated by varying the resonance parameters $\Upsilon(5S)$ and $\Upsilon(6S)$ within $\pm1\sigma$. The final systematic uncertainty is estimated by adding a coherent amplitude ($A_{con} \cdot e^{i\phi'}$) to the fit function. The changes of the resonance parameters and

branching fractions are taken as the systematic uncertainty. The details are listed in Table II.

TABLE II. Summary of the absolute systematic uncertainties in branching fractions (in 10^{-3}) from fitting to the cross sections, where $\mathcal{B}(5,6S)$ represent $\mathcal{B}(\Upsilon(5,6)S)\to\pi^+\pi^-\pi^0\chi_{bJ}$.

$\pi^+\pi^-\pi^0\chi_{bJ}$	$\mathcal{B}(5S)$	$\mathcal{B}(6S)$
BW parametrization	0.1	0.2
PHSP factor	0.1	0.1
Resonance parameters	0.4	0.8
Fit model	2.0	6.0
Sum	2.0	6.1

By using $\mathcal{B}(\Upsilon(5S)\to e^+e^-)=(6.1\pm1.6)\times10^{-6}$ and $\mathcal{B}(\Upsilon(6S)\to e^+e^-)=(2.1^{+1.1}_{-0.6})\times10^{-6}$ [21], we obtain $\mathcal{B}(\Upsilon(5S)\to\pi^+\pi^-\pi^0\chi_{bJ})=(2.5\pm0.6\pm2.0\pm0.7)\times10^{-3}$, $\mathcal{B}(\Upsilon(6S)\to\pi^+\pi^-\pi^0\chi_{bJ})=(8.7\pm4.3\pm6.1^{+4.5}_{-2.5})\times10^{-3}$, where the first errors are statistical, the second are systematic errors combined from the cross sections measurement and line shape fit, and the third result from the branching fractions of $\Upsilon(5S)$ and $\Upsilon(6S)\to e^+e^-$.

To reconstruct $e^+e^-\to\phi\chi_{bJ}$, we require at least two kaons in one event. There is no requirement on the number of photons, but a list of photon candidates is created for the events with photons satisfying $|M(\gamma\gamma_2)-m_{\pi^0}|>13$ MeV/c^2, where γ_2 is the second photon in the event with $E_{\gamma_2}>0.1$ GeV, and m_{π^0} is the nominal mass of π^0. The data are divided into two categories, one where events with one of the photons in the above list satisfies $M(\gamma K^+K^-)_{\rm recoil}\in[9.42,\ 9.50]$ GeV/c^2, i.e., in the $\Upsilon(1S)$ mass region, used to tag $\chi_{bJ}\to\gamma\Upsilon(1S)$ events, the other including all other events, used to tag $\chi_{bJ}\to$non-$\gamma\Upsilon(1S)$ events.

We use the figure of merit, $\mathcal{S}/\sqrt{\mathcal{S}+\mathcal{B}}$, to optimize the ϕ signal window requirement, where $\mathcal{S}$ is the reconstructed number of signal events obtained from MC simulation in the signal region, [9.88, 9.93] GeV/c^2, normalized to the theoretical branching fraction of $\Upsilon(6S)\to\phi\chi_{bJ}$ [16], and $\mathcal{B}$ is the number of background events in the signal region in the $\Upsilon(5S)$ generic MC sample with the c.m. energy shifted to 11.022 GeV. For the first category, we require $M(K^+K^-)$ within $m_\phi\pm7.5$ MeV/c^2, and for category two, we require $M(K^+K^-)$ within $m_\phi\pm7.0$ MeV/c^2, where m_ϕ is the nominal mass of ϕ [21]. The ϕ mass sideband region is defined as $M(K^+K^-)\in[1.000,\ 1.005]$ or $[1.035,\ 1.040]$ GeV/c^2. There is no evidence for peaking background using the ϕ mass sideband events, nor in the generic MC sample mentioned above.

After applying all the selection criteria, the recoil mass spectra of ϕ from both data categories are shown in Fig. 3 for combined data in energy region $\sqrt{s}=10.96$—11.05 GeV. We perform a simultaneous unbinned maximum likelihood fit to the mass spectra with the signals described using MC simulated shapes and a background shape obtained by summing up the expected background shapes at each individual energy point normalized to the luminosity. The expected background shape is obtained from $\Upsilon(5S)$ on-resonance data, where, in calculating the K^+K^- recoil mass, the c.m. energy is changed to that of each individual data point. The ratios of the numbers of χ_{bJ} in the two categories are fixed according to the expected branching fractions [21] and efficiencies. The fit results, which yield $\chi^2/{\rm ndf}=104.2/55=1.9$, are shown in Fig. 3. According to the fit, $(1.5\pm0.5)\times10^3$ χ_{b1} and $(2.4\pm0.5)\times10^3$ χ_{b2} events are produced. The statistical significances are found to be 3.3σ and 4.8σ for χ_{b1} and χ_{b2}, respectively.

When we vary the background shape by multiplying the nominal background shape with a first, second, or third order polynomial, the smallest significances of the χ_{b1} and χ_{b2} signals are found to be 2.6σ and 2.1σ, respectively. The most conservative upper limits on the numbers of produced signal events in all the above tests are reported. After considering the systematic uncertainty which we discuss later, the upper limits for the produced numbers of $\phi\chi_{b1}$ and $\phi\chi_{b2}$ signal events are determined to be 2.0×10^3 and 3.1×10^3 at 90% confidence level (C.L.), respectively, corresponding to upper limits of the Born cross sections of $e^+e^-\to\phi\chi_{b1}$ and $\phi\chi_{b2}$ as 0.6 and 1.0 pb, respectively, averaged over the $\Upsilon(6S)$ region, specifically $\sqrt{s}=10.96$—11.05 GeV.

The sources of systematic uncertainties in the $\phi\chi_{bJ}$ cross section measurement are similar to the $\pi^+\pi^-\pi^0\chi_{bJ}$ modes, including the tracking efficiency, PID, photon detection, luminosity, trigger simulation, ISR correction, ϕ mass window, and corresponding branching fraction. Most of these have been discussed in the $\pi^+\pi^-\pi^0\chi_{bJ}$ analysis. The uncertainties from the ϕ mass window requirement is found to be negligible by studying the consistency of the K^+K^- invariant mass between data and MC simulation. The uncertainty from the branching fraction of $\phi\to K^+K^-$ is 1.0% [21]. The total systematic uncertainty for the cross section measurement is thus, combining all uncertainties in quadrature, 5.5% for both modes.

In summary, using the energy scan data in the vicinity of the $\Upsilon(6S)$ resonance, we observe $e^+e^-\to\pi^+\pi^-\pi^0\chi_{b1}$ and find evidence of $e^+e^-\to\omega\chi_{b2}$ with statistical significances of 6.1σ and 4.0σ, respectively. The limited statistics prevents us from drawing conclusion concerning the origin of the signal events, that is, whether they arise from bottomonium decay, continuum production, or both. Since all the known final states with bottomonium observed so far come from excited bottomonium decay, we assume these final states have the same origin. Thus the corresponding branching fractions can be estimated, where $\mathcal{B}(\Upsilon(5S)\to\pi^+\pi^-\pi^0\chi_{bJ})=(2.5\pm0.6\pm2.0\pm0.7)\times10^{-3}$ is consistent with the previous measurement [4], and $\mathcal{B}(\Upsilon(6S)\to\pi^+\pi^-\pi^0\chi_{bJ})=(8.7\pm4.3\pm6.1^{+4.5}_{-2.5})\times10^{-3}$, which is consistent with the theoretical predictions [16], is measured for the first time. The processes $e^+e^-\to\phi\chi_{bJ}$ are also searched for in data within $\sqrt{s}=10.96$—11.05 GeV, with no significant signals being observed. We report upper limits on the Born cross sections of $e^+e^-\to\phi\chi_{b1}$ and $\phi\chi_{b2}$ are 0.6 and 1.0 pb at 90% C.L., respectively. Compared with the total cross section of $e^+e^-\to\Upsilon(6S)$, these upper limits correspond to $\Upsilon(6S)$ decay branching fractions of order 10^{-3}, well above the theoretical predictions of order 10^{-6} [16].

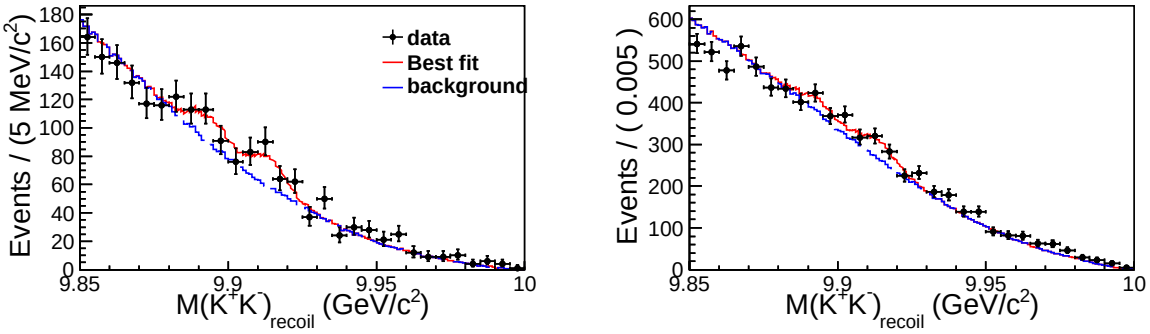

FIG. 3. The simultaneous fit results for data having $M(\gamma K^+K^-)$ in the $\Upsilon(1S)$ mass window (left) and out (right). Dots with error bars are data, the red solid lines are the best fit, and blue dashed lines are backgrounds.

We thank Dr. K. Li for his fantastic idea and kindly help. We thank the KEKB group for excellent operation of the accelerator; the KEK cryogenics group for efficient solenoid operations; and the KEK computer group, the NII, and PNNL/EMSL for valuable computing and SINET5 network support. We acknowledge support from MEXT, JSPS and Nagoya's TLPRC (Japan); ARC (Australia); FWF (Austria); NSFC and CCEPP (China); MSMT (Czechia); CZF, DFG, EXC153, and VS (Germany); DST (India); INFN (Italy); MOE, MSIP, NRF, RSRI, FLRFAS project and GSDC of KISTI (Korea); MNiSW and NCN (Poland); MES and RFAAE (Russia); ARRS (Slovenia); IKERBASQUE and MINECO (Spain); SNSF (Switzerland); MOE and MOST (Taiwan); and DOE and NSF (USA).

[1] Y. P. Kuang, Front. Phys. China **1**, 19 (2006).
[2] K.-F. Chen *et al.* [Belle Collaboration], Phys. Rev. Lett. **100**, 112001 (2008).
[3] I. Adachi *et al.* [Belle Collaboration], Phys. Rev. Lett. **108**, 032001 (2012).
[4] X. H. He *et al.* [Belle Collaboration], Phys. Rev. Lett. **113**, 142001 (2014).
[5] A. Bondar *et al.* [Belle Collaboration], Phys. Rev. Lett. **108**, 122001 (2012).
[6] P. Krokovny *et al.* [Belle Collaboration], Phys. Rev. D **88**, 052016 (2013).
[7] A. Garmash *et al.* [Belle Collaboration], Phys. Rev. D **91**, 072003 (2015).
[8] K.-F. Chen *et al.* [Belle Collaboration], Phys. Rev. D **82**, 091106 (2010).
[9] R. Mizuk *et al.* [Belle Collabration], Phys. Rev. Lett. **117**, 142001 (2016).
[10] A. Ali, C. Hambrock and M. J. Aslam, Phys. Rev. Lett. **104**, 162001 (2010).
[11] N. Brambilla *et al.*, Eur. Phys. J. C **74**, 2981 (2014).
[12] M. B. Voloshin, Phys. Rev. D **85**, 034024 (2012).
[13] F. K. Guo, U. G. Meissner and C. P. Shen, Phys. Lett. B **738**, 172 (2014).
[14] X. Li and M. B. Voloshin, Phys. Rev. D **90**, 014036 (2014).
[15] D. Y. Chen, X. Liu and T. Matsuki, Phys. Rev. D **90**, 034019 (2014).
[16] Q. Huang, B. Wang, X. Liu, D. Y. Chen and T. Matsuki, Eur. Phys. J. C **77**, 165 (2017).
[17] D. Santel *et al.* [Belle Collaboration], Phys. Rev. D **93**, 011101 (2016).
[18] S. Kurokawa and E. Kikutani, Nucl. Instrum. Methods Phys. Res., Sect. A **499**, 1 (2003), and other papers included in this volume; T. Abe, *et al.*, PTEP **2013**, 03A001 (2013), and following articles up to 03A011.
[19] A. Abashian *et al.* [Belle Collaboration], Nucl. Instrum. Methods Phys. Res., Sect. A 479, 117 (2002); also see detector section in J. Brodzicka *et al.* [Belle Collaboration], PTEP **2012**, 04D001 (2012).
[20] D. J. Lange, Nucl. Instrum. Meth. A **462**, 152 (2001).
[21] C. Patrignani *et al.* [Particle Data Group], Chin. Phys. C, **40**, 100001 (2016).
[22] E. A. Kuraev and V. S. Fadin, Sov. J. Nucl. Phys. **41**, 466 (1985).
[23] S. Actis *et al.*, Eur. Phys. J. C **66**, 585 (2010).